ACS APPLIED MATERIALS & INTERFACES

Research Article

www.acsami.org

Existence of a Lower Critical Radius for Incorporation of Silica Particles into Zinc during Electro-codeposition

Tabrisur R. Khan,[†] Ashokanand Vimalanandan,[†] Frank Marlow,[‡] Andreas Erbe,[†] and Michael Rohwerder*[,†]

[†]Max-Planck-Institut für Eisenforschung GmbH, Max-Planck-Straße 1, 40237 Düsseldorf, Germany

[‡]Max-Planck-Institut für Kohlenforschung, Kaiser-Wilhelm-Platz 1, 45470 Mülheim an der Ruhr, Germany

ABSTRACT: Recently, it was shown that the surface modification of silica particles with −SH functional groups enables their electro-codeposition with zinc. Here, however, we report that no incorporation into Zn can be observed for such modified particles with diameters of <100 nm, while incorporation is possible for particles with diameters of 225 nm and larger. Furthermore, when silica particles are functionalized with mixtures of −SH and −Cl functional groups, which affect the interface energy at the particle/metal interface differently but have similar interfacial energies for the particle/electrolyte interface, it is found that, for successful incorporation of the particles, a minimum amount of −SH functional groups is needed. An explanation for these observations has been derived based on energetic considerations regarding the interfaces involved in the process.

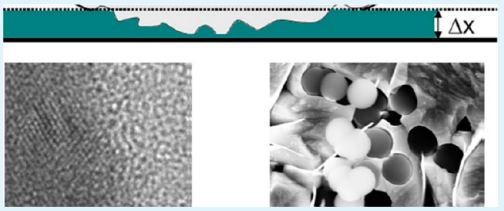

KEYWORDS: *composite coating, corrosion protection, metallic coating, thin film, sacrificial coating, interfacial energy*

1. INTRODUCTION

Coatings play an important role in corrosion protection of metals. Organic coatings, as well as inorganic and metallic coatings, are used, often in combination. In recent years, because of steadily increasing requirements, such as the formability of precoated metal, which leads to unavoidable defects in the coating,[1] a strong demand for so-called "self-healing coatings" has led to intense research on that subject, usually with a focus on inorganic coatings (such as sol−gel) or organic coatings.[2−11] Metallic coatings have been widely neglected so far, although, for instance, standard zinc coatings for cathodic protection already do provide some degree of self-healing, which can be enhanced by alloying.[12] More-flexible approaches than just alloying can be only achieved by incorporating suitable nanocontainers into the metal matrix. Composite coatings on a metallic basis have already been prepared in the past, e.g., to enhance mechanical, physical, and tribological properties, and also the corrosion resistance.[13−20] Composite coatings have also been proposed as electrocatalysts, photoelectrocatalysts, or photoelectrochromic materials.[17]

Despite the large technological importance in corrosion protection, only very few composite coatings that are based on based on Zn have been prepared, because of the difficulties involved in incorporating particles into the metal matrix.[13,21−26] Silica is one of the most promising materials for the storage of active agents to be incorporated into zinc for enhancing its protective properties against corrosion, because of its stability at acidic pH and instability in alkaline pH. Recently, a concept of "self-healing" coatings using mesoporous silica incorporated into zinc has been proposed for corrosion inhibition of steel sheet at the cut edge.[27] Industrial Zn electrodeposition is usually carried out at pH 1.8−2, where silica is stable. On the steel surface at the cut edge, on the other hand, alkaline pH prevails and the silica particles decompose, releasing the stored substances.[27] However, unlike other oxides, the incorporation of silica into metals in general, and especially into zinc, during electro-codeposition at low pH is very limited.[13,28,29] Electro-codeposition of oxide particles into the metal matrix is a very complex phenomenon. The incorporation of nanoparticles into the metal matrix depends on many process parameters, as discussed in the literature.[19,20] The transport of particles toward the electrode via convection and diffusion is well-understood.[30] Particle concentration, as well as the surface charge, type, shape, and size of the particles also affect the degree of particle incorporation.[19,20,31]

Furthermore, the role of the forces that are acting between the particle and the electrode has been discussed.[26,30,32−34] One early suggestion was that, when touching the electrode, the particles become mechanically entrapped.[35] Later, electrostatic interactions between the electrode and the surface charge of the particles were considered to be the main determining factor for particle incorporation.[30,32,36] More recent works on the incorporation of $Al_2O_3/TiO_2/SiO_2$ into Cu and Ni seem to favor the concept of the electrostatic force.[14−16,36] However, the argumentations based on electrostatic force considerations were questioned in other works (see, for example, the work of Khan et al.[26]). More convincing seems to be the role of interface energies. For incorporation, the interface energy between the particle and the electrolyte should be greater than

Received: August 29, 2012
Accepted: October 29, 2012
Published: October 29, 2012

that observed between the particle and the metal matrix.[37] For instance, hydrophilic particles have been shown to be pushed away by the growing metal matrix, which contradicts the above concept, based on the electrostatic force, and points toward making particles more hydrophobic for incorporation.[33,37,38]

However, making the particles more hydrophobic also interferes with their dispersion into the galvanizing bath. Recently, it was shown that focusing on decreasing the interface energy between the particle and the metal is a promising way to incorporate silica particles into Zn.[26] It was shown that incorporation at low pH is possible after modification of the particle surface with thiol functional groups. Unmodified SiO_2 particles, or particles modified with a −Cl group, have not been found to be incorporated into Zn.[26] Because −Cl- and −SH-terminated surfaces show virtually the same contact angles and critical surface tensions,[39−42] −SH groups have been proposed to substantially decrease the particle/metal interface energy via the formation of bonds with the growing metal.[26] This previous study was performed exclusively with particles of one specific diameter of 225 nm.[26]

In the initial stages of particle incorporation into a growing metal, the contribution of the metal/particle interface to the total free energy of the system is given by the product of the area in contact with the metal and the particle/metal interface energy. The initial contact area is expected to scale with the diameter of the particles. Only brief discussions on the effect of particle size on codeposition have been given.[19,20,31] Moreover, the critical particle sizes reported in the literature range over several orders of magnitude.[20,43−46]For instance, comparing 20-nm and 2-μm SiO_2 for deposition with Zn, the weight fraction of the smaller particles was lower than that of the larger particles.[46] An experimental and theoretical analysis of the dependence on the diameter of SiO_2 incorporated into Zn is the first subject of this work.

Furthermore, the particle/metal interface energy is also affected by the number of modifying functional groups on the surface of the SiO_2 particle. However, to the best knowledge of the authors, there is no report on the effect of the density of functional groups on particle surface on codeposition, especially in terms of interfacial energy. Hence, as a second subject of this work, the codeposition behavior of particles with mixtures of −Cl and −SH functional groups on the surface is studied to elucidate the effect of the density of groups modifying the metal/particle interface energy alone without altering the particle/electrolyte interfacial energy.

2. EXPERIMENTAL SECTION

2.1. Materials. Thiol-modified particles (SiO_2−SH) with diameters of 97 nm and 1.7 μm were purchased from Microparticles GmbH. All chemicals—$ZnSO_4{\cdot}7H_2O$ (Sigma−Aldrich), tetraethoxysilane (TEOS, Fluka), ammonia solution (28%−30%, Merck), ethanol (absolute reagent type, Merck), 3-mercaptopropyltrimethoxysilane (MPTMS, Aldrich), and 3-chloropropyltrimethoxysilane (CPTMS, Aldrich) were used as purchased.

2.2. Stöber Silica. Silica particles of different sizes were synthesized using the Stöber process.[47] In a typical synthesis process, TEOS was added to the basic ethanol−water mixture. After 2 h, the particles were separated from the solution using a centrifuge. Details about the amounts are given in Table 1.

2.3. Modification of Silica. Modification of SiO_2 particles was performed according to standard procedures.[48] Two milliliters (2 mL) of the functionalization agent (CPTMS/MPTMS) were added to a solution containing 100 mg of SiO_2 dispersed in 100 mL of an ethanol−water mixture (95/5, w/w). When functionalization with a mixture of two functional groups was carried out, different volume ratios of CPTMS and MPTMS were mixed prior to addition to the solution. The solution was stirred for a day and the particles were separated from the solution by centrifugation at 5000 rpm. The particles were then washed with water three times before they were dispersed into electrolyte for electro-codeposition.

Table 1. Chemical Composition for the Synthesis of Silica Particles of Different Sizes

volume of ethanol/NH_3 solution/water/TEOS (mL)	mole fraction of ethanol:NH_3:water:TEOS	average particle diameter (from SEM) (nm)
328.75/16.75/123.3/31.25	0.608:0.006:0.379:0.007	225
274/208/123.3/31.25	0.083:0.111:0.798:0.008	700

The prepared particles are referred to as SiO_2−Cl for purely Cl-terminated particles, SiO_2−SH:Cl (1:1) for a volume ratio MPTMS:CPTMS of 1:1 and SiO_2−SH:Cl (3:7) for a volume ratio MPTMS:CPTMS 3:7. Within the limit of the experimental error, the volume ratio is identical to the molar ratio in a liquid mixture. Because no exchange reactions are expected on the surface for silanes, the surface composition of the final modified surface should be reflected by the bulk composition of the reactants, if reactants with the same reactivity toward condensation and surface binding (given by the group R in $-Si(-OR)_3$) are used, as is the case in this study.

2.4. Electro-codeposition. For electro-codeposition, 1.2 M $ZnSO_4$ was used as the electrolyte. For the codeposition, 150 mg of the modified silica particles were added into 10 mL of electrolyte. Potentiostatic electro-codeposition was carried out in a conventional three-electrode cell at −1.2 V against a Ag/AgCl/3 M KCl reference electrode. Stainless steel bars with dimensions of ∼4 cm × 1.5 cm × 1 mm were used as working electrodes. Prior to use as working electrodes, the bars were ground with 1000 grade SiC grinding paper, followed by cleaning with ethanol and water in an ultrasonic bath.

2.5. Analysis. The Zeiss Leo 1550VP field-emission scanning electron microscopy (FE-SEM) system was operated at 11 kV to obtain SEM images. As shown previously, adsorbed insulating particles are visible in SEM images as bright features, while particles in close contact with the metal matrix appear dark.[21]

High-resolution TEM (HRTEM) imaging was performed using a JEOL JEM-2200 FS microscope operated at 200 kV. A Zeiss Model 1540 XB focused-ion-beam (FIB) system with a Ga^+ ion accelerating voltage of 30 kV was used to prepare the TEM specimen. A TEM sample with dimensions of ∼25 μm × 25 μm × 0.1 μm was prepared so that the sample plane remained parallel to the polishing plane.

The modified SiO_2 particles were analyzed via X-ray photoelectron spectroscopy (XPS), using a Physical Electronics Quantum 2000 Scanning ESCA Microprobe. Sample preparation for XPS was done by pressing the modified silica particles into an indium foil. Each analysis started with a survey scan from 0 to 1100 eV with a dwell time of 100 ms, with a pass energy of 93.9 eV at steps of 0.287 eV with 5 sweeps. During acquisition of detailed spectra, the pass energy was set to 23.2 eV at steps of 0.287 eV with 40 sweeps. CasaXPS software was used to analyze the data.

3. RESULTS AND DISCUSSION

3.1. Size Dependence of Particle Incorporation. *3.1.1. Results for Modified and Unmodified SiO_2 Particles.* SiO_2 particles of different sizes (225 nm, 700 nm, and 1.7 μm) were codeposited with zinc at pH 3. Figures 1a and 1b show SEM images of zinc-plated samples, where zinc was electro-deposited in the presence of silica particles with diameters of 700 nm and 1.7 μm at pH 3. Particles of all sizes (225 nm to 1.7 μm) were just adsorbed on the coating surface. No partially incorporated particles have been observed. Hence, it is concluded that no particle incorporation occurs.

The situation changes when SiO_2−SH particles of different diameters ranging from 97 nm to 1.7 μm were present in the

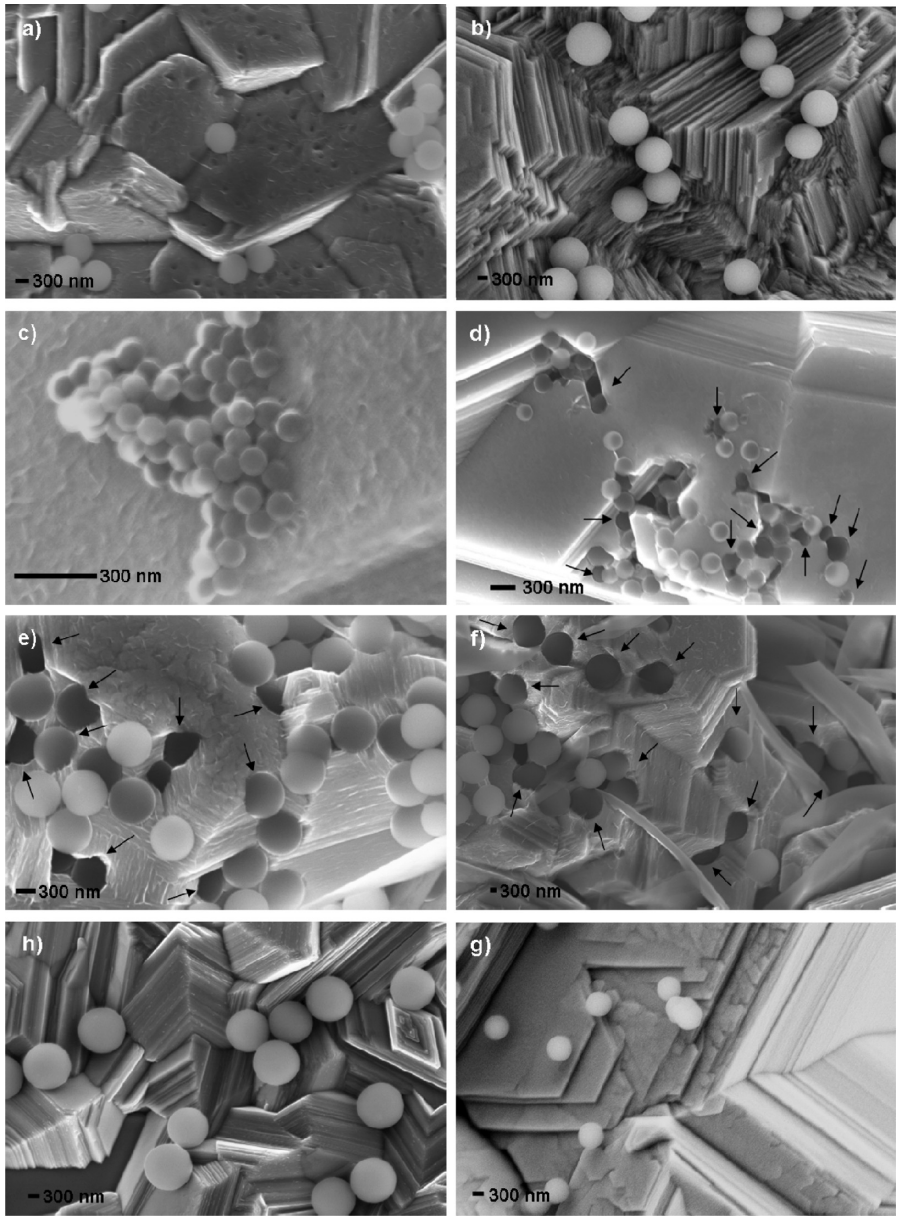

Figure 1. SEM micrographs of Zn deposited in the presence of (a) 700-nm SiO_2 particles and (b) 1.7-μm SiO_2 particles. SEM images of Zn-SiO_2 composite coatings prepared using SiO_2−SH particles with diameters of (c) 97 nm, (d) 225 nm, (e) 700 nm, and (f) 1.7 μm. SEM images of Zn electrodeposited in the presence of SiO_2−Cl particles with diameters of (h) 700 nm and (g) 1.7 μm. All the depositions were carried out at pH 3. Arrows point to partially incorporated particles.

deposition bath. The resulting surface morphologies are depicted in Figures 1c−f.

Partially incorporated particles are observed using SEM when particles with diameters of 225 nm or larger were used in the deposition bath (see Figures 1d−f). However, no incorporation was observed for particles that are only 97 nm in diameter (Figure 1c). These particles are only adsorbed on the zinc surface, similar to unmodified particles. No incorporation was observed either when the particles were just modified with Cl-groups (see Figures 1h and 1g).

SiO_2−SH particles 180 nm in diameter were also codeposited with zinc (see Figure 2). Incorporation of particles has not been observed. This result indicates that SiO_2−SH particles with diameters of <180 nm do not incorporate inside the zinc matrix. Hence, there must be a critical diameter above which SiO_2−SH particles become incorporated inside the zinc matrix.

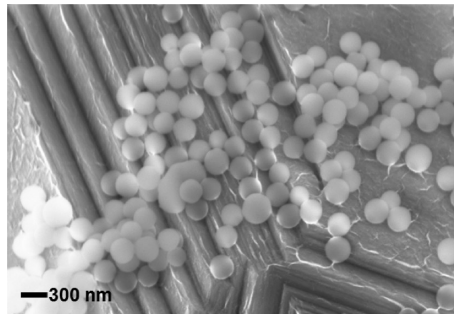

Figure 2. SEM micrograph of Zn-SiO_2 coating prepared using SiO_2−SH particles 180 nm in diameter at pH 3.

dx.doi.org/10.1021/am301821m | ACS Appl. Mater. Interfaces 2012, 4, 6221−6227

3.1.2. Particle/Zinc Interface. Figure 3 shows an HRTEM micrograph at the SiO_2/Zn interface of a sample that was

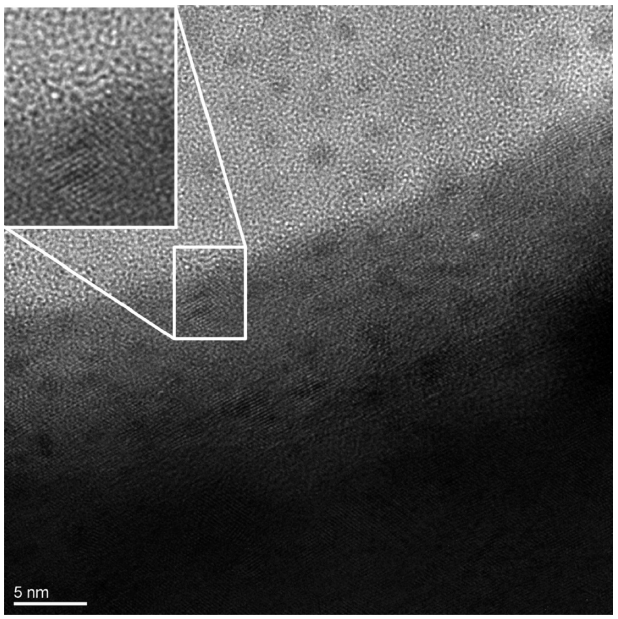

Figure 3. HRTEM micrograph at the SiO_2/Zn interface. The upper part (lighter color) shows the silica particle, and the lower part shows the zinc matrix. The enlarged area shows how the amorphous silica and the crystalline zinc meet without a gap between them.

prepared via the electro-codeposition of SiO_2−SH particles 225 nm in diameter with zinc. The HRTEM micrograph reveals that there is no cavity between the particle and the zinc matrix. This result indicates that, when incorporation occurs, direct contact between the silica and the metal is established.

3.1.3. Discussion of Size Dependence. To summarize the above results, no particle incorporation was observed for unmodified SiO_2 and SiO_2−Cl particles of any size. Only SiO_2−SH particles with diameters of 225 nm and larger can be incorporated. The incorporation of SiO_2−SH has previously been explained as being due to the decrease of the interfacial energy of the metal/SiO_2 interface, because of the surface modification.[26] In general, modification of the surface of the particles causes changes in the interface energies σ. For a more-detailed analysis, the interfacial energy of the particle/electrolyte interface ($\sigma_{P/E}$) and of the particle/metal interface ($\sigma_{P/M}$) will be considered, because they play a vital role in the incorporation of particles into metal. Thermodynamically, the incorporation of particles into the metal matrix is favorable if $\sigma_{P/E}$ is large, which can be realized by making particles hydrophobic.[37,49] However, the dispersibility of hydrophobic particles in aqueous electrolytes sets a limit in the application.[49] For SiO_2−Cl particles, $\sigma_{P/E}$ increases compared to unmodified SiO_2, but not to an extent sufficient to achieve particle incorporation. As a result, only adsorption takes place. On the other hand, for SiO_2−SH, $\sigma_{P/E}$ is increased, compared to SiO_2 particles, by virtually the same amount as that for SiO_2−Cl, because both possess similar contact angles and critical surface tensions.[39−42] In addition, for SiO_2−SH, $\sigma_{P/M}$ is also lowered, because of a strong interaction of the functional groups with the metal.[50] As shown previously, the reduction of $\sigma_{P/M}$ leads to incorporation of particles into the metal matrix.[26]

The experimental results presented here indicate that SiO_2−SH can be incorporated only above a certain diameter. It is proposed that this critical incorporation diameter exists because of differences in the number of functional groups directly interacting with the growing zinc surface during electrodeposition for particles with different diameters.

Consider the total area A_0 of the particle,

$$A_0 = \pi d^2$$

where d is its diameter. In the initial stage of particle incorporation, only a cap of height $h = \Delta x$ with surface area $\pi d\Delta x$ is inside the metal matrix. The projected area on the metal surface is

$$\pi a^2 = \pi\left[\frac{d^2}{4} - \left(\frac{d^2}{4} - \Delta x^2\right)\right]$$

with a being the radius of the projection circle. The situation is depicted in Figure 4.

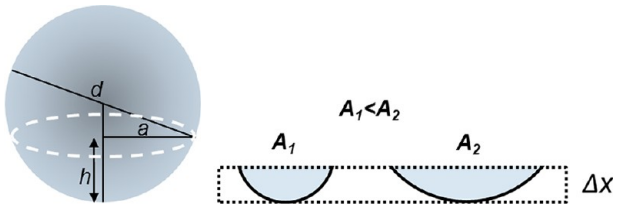

Figure 4. (Left) Depiction of a particle as a sphere with diameter d; h is the height of the cap. (Right) Scheme of two particles, having different areas A_1 and A_2, approaching the cathode; Δx represents the growth of the zinc layer on the cathode during the initial phase of codeposition.

The overall energy change (ΔE_i) for this initial incorporation step will then be

$$\Delta E_i = \pi d\Delta x(\sigma_{P/M} - \sigma_{P/E}) - \pi a^2 \sigma_{M/E}$$

with the interface tension $\sigma_{M/E}$ between metal and electrolyte. For incorporation to occur, $\Delta E_i < 0$; hence,

$$\pi d\Delta x(\sigma_{P/M} - \sigma_{P/E}) - \pi\left[\frac{d^2}{4} - \left(\frac{d}{2} - \Delta x\right)^2\right]\sigma_{M/E} \leq 0$$

Solving for d yields, as a condition for incorporation,

$$d \geq \Delta x\left(\frac{\sigma_{M/E}}{\sigma_{P/E} - \sigma_{M/E} - \sigma_{P/M}}\right) \quad (1)$$

Although full incorporation is only to be expected for $\sigma_{P/M} < \sigma_{P/E}$, according to this equation, initial stage incorporation is even possible, if $\sigma_{P/M} > \sigma_{P/E}$, as long as $\sigma_{P/M} < \sigma_{P/E} + \sigma_{M/E}$, which means that no gap between silica and zinc will form, in accordance with observations made via HTREM (see Figure 3).

However, it is to be expected that as soon as the zinc deposition proceeds further, the particle would be squeezed out of the matrix, because, above a certain stage Δx, it will not longer fulfill eq 1. However, the prepared particles do possess a certain surface roughness. If the initial stage incorporation Δx is large enough, the particle will be held tightly by mechanical interdigitation with the zinc layer, i.e., for $\Delta x > \Delta x_{crit}$, where Δx_{crit} is the corresponding minimum incorporation depth for interdigitation. The particle then will continue to be

incorporated. This will be the case for all particles with a d value such that

$$d \geq d_{crit} = \Delta x_{crit}\left(\frac{\sigma_{M/E}}{\sigma_{P/E} - \sigma_{M/E} - \sigma_{P/M}}\right) \quad (2)$$

and if $\sigma_{P/M} < \sigma_{P/E} + \sigma_{M/E}$.

Because most of the interfacial energies are difficult to determine precisely, and Δx_{crit} is also not known, the exact magnitude of the d_{crit} is difficult to obtain from pure theoretical considerations. However, it is suggested that Δx_{crit} will be at least slightly larger than the surface roughness of the particle, in order to enable the proposed interdigitation.

Additional factors may play a role, especially the interaction time of the particles with the surface in relation to the deposition rate, but also diffusion and hydrodynamic effects may affect whether mechanical interdigitation will occur. From the experimental results obtained here, it is concluded that, in the case investigated here (i.e., for SiO_2−SH particles), 97 nm < d_{crit} < 225 nm.

The result just derived not only shows that, for a successful incorporation of particles into the metal matrix, the particle must have a diameter larger than the critical incorporation diameter, but also give an indication that the interfacial energies are important. The interfacial energies involving the particle are related to the number of functional groups on the particle surface. That leads to the hypothesis that incorporation is also affected by the number of functional groups on the particle surface. This hypothesis has been tested by the preparation of SiO_2 particles whose surface was modified by different mixtures of −Cl and −SH functional groups and subsequent electrocodeposition experiments, as will be described in the next section.

3.2. Variation of the Surface Composition of SiO_2 Particles. *3.2.1. Characterization of the Modified Particles.* XPS was used to characterize the functionalized silica particles. Figure 5 shows the XPS spectra of SiO_2 particles that were functionalized with a mixture of −SH and −Cl functional groups.

Figure 5a shows the core level spectra of sulfur (S 2s and S 2p) and chlorine (Cl 2p) for SiO_2−SH:Cl (1:1). Both S 2s and Cl 2p have almost the same intensity. Because of the inhomogeneity of the photoelectron escape depth of XPS on the nanoparticles, the peak ratio, as typically analyzed for flat interfaces, is rather difficult to interpret. Figure 5b shows the intensities SiO_2−SH:Cl (3:7). The results show a reduction of the sulfur-related peaks relative to the Cl 2p peak, as expected for the lower fraction of −SH in the particle surface.

3.2.2. Effect of Functional Groups during Codeposition. To investigate the effect of the density of functional groups on particle incorporation, experiments were performed with particles modified with both −SH and −Cl groups, described above. For these experiments, three different particle diameters (225, 500, and 700 nm) were chosen. In Figure 6, typical SEM images obtained from the different resulting zinc coatings are shown.

While SiO_2−SH:Cl (1:1) particles with diameters of 500 and 700 nm are incorporated into the zinc metal matrix, in no case has any incorporation been observed for SiO_2−SH:Cl (3:7) particles with diameters of 700 nm as well as for SiO_2−SH:Cl (1:1) particles with diameters of 225 nm.

3.2.3. Discussion of the Effect of Functional Groups on Incorporation. Based on the results shown above, it can be concluded that SiO_2 particles 500 and 700 nm in diameter covered with at least 50% −SH will be incorporated into zinc. On the other hand, only adsorbed particles are obtained on the zinc surface when SiO_2 particles 225 and 700 nm in diameter, with 50% and 30% or lower −SH coverage, respectively, are used during the deposition. This finding confirms the hypothesis stated in section 3.1.3 and can be explained in terms of the interfacial energies. Modification of the particles with different functional groups changes the interfacial energies ($\sigma_{P/M}$ and $\sigma_{P/E}$). When the particles 500 and 700 nm in diameter are covered with at least 50% −SH functional groups, $\sigma_{P/M}$ becomes sufficiently lower, compared to unmodified particles, because of the bond formation of −SH with the metal, which leads to incorporation of the particles into the metal matrix. When the particles 225 and 700 nm in diameter are covered with 50% and 30% or less −SH functional groups, respectively, $\sigma_{P/M}$ is not sufficiently reduced to enable the incorporation of particles. This result also indicates that the critical number of −SH functional groups required for incorporation of the 700-nm-diameter SiO_2 particles lies between 30% and 50% coverage.

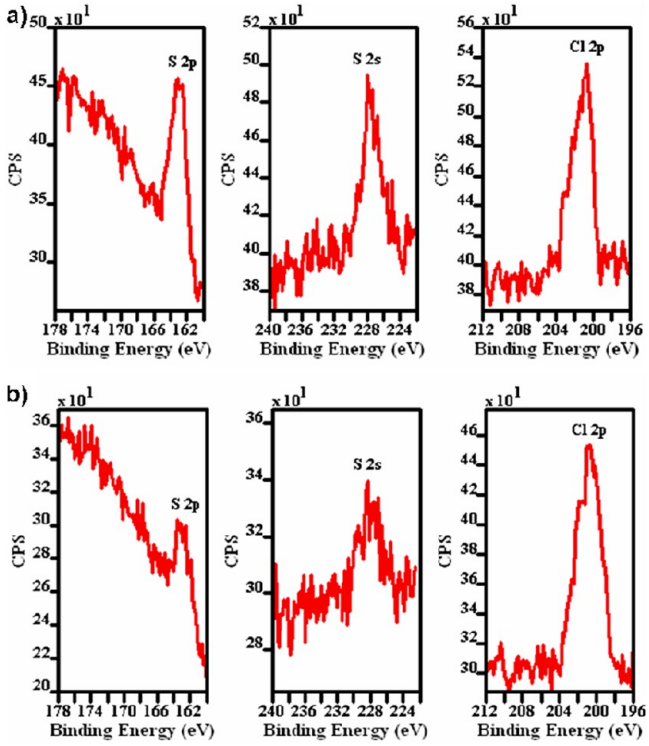

Figure 5. X-ray photoelectron spectroscopy (XPS) spectra of (a) SiO_2−SH:Cl (1:1) and (b) SiO_2−SH:Cl (3:7).

The results of the 700-nm SiO_2 particles functionalized with − Cl/−SH or a combination of both are summarized in the scheme shown in Figure 7.

4. CONCLUSIONS

In this paper, it was shown that, for the incorporation of −SH-modified silica particles into zinc, a critical diameter exists below which no incorporation can occur. This is explained by the need of a mechanical interdigitation of zinc and silica, because, supposedly, the interfacial energy between zinc and the particle is not lowered enough to fulfill $\sigma_{P/M} < \sigma_{P/E}$. Incorporation then is still possible for particles with a diameter d larger than a critical diameter d_{crit}:

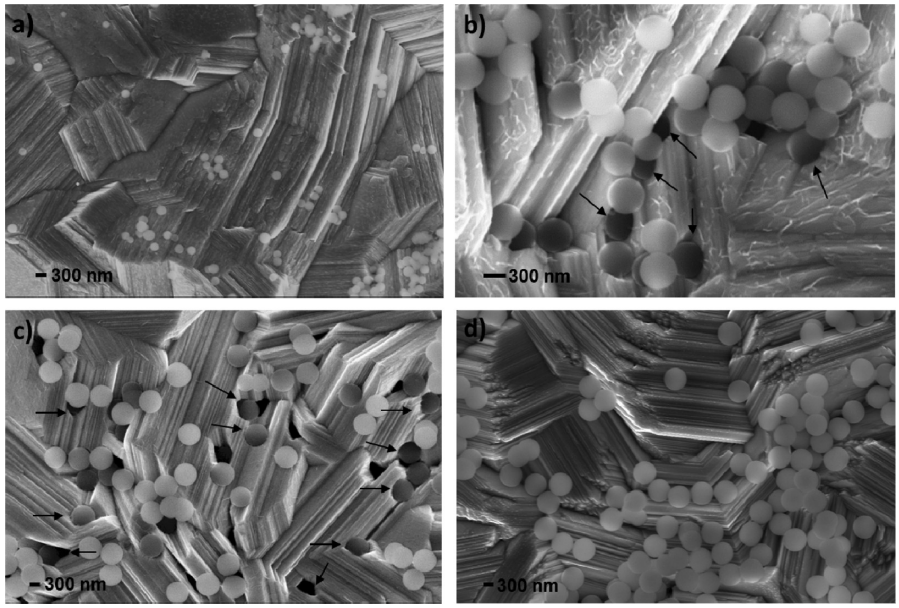

Figure 6. SEM images of zinc coatings prepared in the presence of SiO_2−SH:Cl (1:1) particles with diameters of (a) 225 nm, (b) 500 nm, and (c) 700 nm, respectively, and (d) SiO_2−SH:Cl (3:7) particles with diameters of 700 nm.

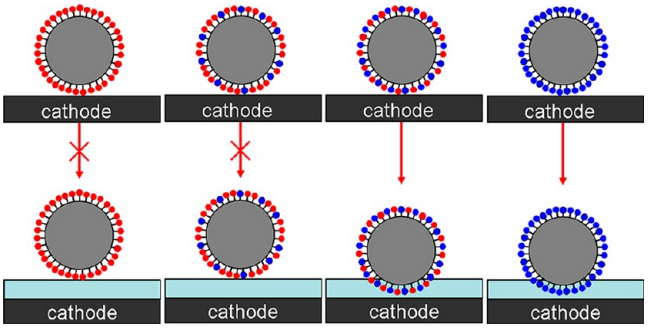

Figure 7. Schematic shows the role of the density of functional groups on the particle surface during electro-codeposition. The blue and red circles symbolize −SH and −Cl functional groups, respectively.

$$d > d_{crit} = \Delta x_{crit}\left(\frac{\sigma_{M/E}}{\sigma_{P/E} - \sigma_{M/E} - \sigma_{P/M}}\right)$$

as long as $\sigma_{P/M} < \sigma_{P/E} + \sigma_{M/E}$, which was also supported by HTREM images. The critical incorporation depth (Δx_{crit}) is suggested to be at least slightly larger than the surface roughness of the particles. It is proposed that, also, for other cases where observations of a minimum particle diameter for incorporation into a metal have been made,[44,46] the same explanation is valid. Furthermore, we have shown that the interfacial energy ($\sigma_{P/M}$) can be directly tuned by controlling the degree of functional −SH groups.

AUTHOR INFORMATION

Corresponding Author

*Tel.: +49 211 6792-442 /-914. Fax: +49 211 6792-218. E-mail: rohwerder@mpie.de.

Notes

The authors declare no competing financial interest.

ACKNOWLEDGMENTS

T.R.K. acknowledges a scholarship from ThyssenKrupp Steel Europe in the framework of the IMPRS-SurMat and support from ASKORR, an FHG-MPG cooperative project. The authors acknowledge Prof. Stratmann for fruitful discussions and support.

REFERENCES

(1) Baumert, B.; Stratmann, M.; Rohwerder, M. *Z. Metallkd.* **2004**, *95* (6), 447−455.
(2) White, S. R.; Sottos, N. R.; Geubelle, P. H.; Moore, J. S.; Kessler, M. R.; Sriram, S. R.; Brown, E. N.; Viswanathan, S. *Nature* **2001**, *409* (6822), 794−797.
(3) Paliwoda, G.; Stratmann, M.; Rohwerder, M.; Potje-Kamloth, K.; Lu, Y.; Pich, A. Z.; Adler, H.-J. *Corros. Sci.* **2005**, *47* (12), 3216−3233.
(4) Rohwerder, M.; Michalik, A. *Electrochim. Acta* **2007**, *53* (3), 1300−1313.
(5) Rohwerder, M.; Le Minh, D.; Michalik, A. *Electrochim. Acta* **2009**, *54* (25), 6075−6081.
(6) Toohey, K. S.; Sottos, N. R.; Lewis, J. A.; Moore, J. S.; White, S. R. *Nat. Mater.* **2007**, *6* (8), 581−585.
(7) Skorb, E. V.; Fix, D.; Andreeva, D. V.; Möhwald, H.; Shchukin, D. G. *Adv. Funct. Mater.* **2009**, *19* (15), 2373−2379.
(8) Zheludkevich, M. L.; Shchukin, D. G.; Yasakau, K. A.; Möhwald, H.; Ferreira, M. G. S. *Chem. Mater.* **2007**, *19* (3), 402−411.
(9) Shchukin, D. G.; Möhwald, H. *Small* **2007**, *3* (6), 926−943.
(10) Shchukin, D. G.; Sukhorukov, G. B.; Möhwald, H. *Angew. Chem., Int. Ed.* **2003**, *42* (37), 4472−4475.
(11) Borisova, D.; Möhwald, H.; Shchukin, D. G. *ACS Nano* **2011**, *5* (3), 1939−1946.
(12) Krieg, R.; Evers, S.; Schuhmacher, B.; Schauer-Pass, J.; Rohwerder, M. *Corros. Sci.* **2012**, *65*, 119−127.
(13) Azizi, M.; Schneider, W.; Plieth, W. *J. Solid State Electrochem.* **2005**, *9* (6), 429−437.
(14) Bund, A.; Thiemig, D. *Surf. Coat. Technol.* **2007**, *201* (16−17), 7092−7099.
(15) Bund, A.; Thiemig, D. *J. Appl. Electrochem.* **2007**, *37* (3), 345−351.
(16) Podlaha, E. J. *Nano Lett.* **2001**, *1* (8), 413−416.
(17) Musiani, M. *Electrochim. Acta* **2000**, *45* (20), 3397−3402.

(18) de Tacconi, N. R.; Boyles, C. A.; Rajeshwar, K. *Langmuir* **2000**, *16* (13), 5665−5672.
(19) Low, C. T. J.; Wills, R. G. A.; Walsh, F. C. *Surf. Coat. Technol.* **2006**, *201* (1−2), 371−383.
(20) Hovestad, A.; Janssen, L. J. J. *J. Appl. Electrochem.* **1994**, *25* (6), 519−527.
(21) Xia, X.; Zhitomirsky, I.; McDermid, J. R. *J. Mater. Process. Technol.* **2009**, *209* (5), 2632−2640.
(22) Kammona, O.; Kotti, K.; Kiparissides, C.; Celis, J. P.; Fransaer, J. *Electrochim. Acta* **2009**, *54* (9), 2450−2457.
(23) Praveen, B. M.; Venkatesha, T. V.; Naik, Y. A.; Prashantha, K. *Synth. React. Inorg. Met.-Org. Chem.* **2007**, *37* (6), 461−465.
(24) Gomes, A.; Pereira, M. I. D. *Electrochim. Acta* **2006**, *51* (7), 1342−1350.
(25) Gomes, A.; Pereira, M. I. D. *Electrochim. Acta* **2006**, *52* (3), 863−871.
(26) Khan, T. R.; Erbe, A.; Auinger, M.; Marlow, F.; Rohwerder, M. *Sci. Technol. Adv. Mater.* **2011**, *12*, 5.
(27) Stempniewicz, M.; Rohwerder, M.; Marlow, F. *ChemPhysChem* **2007**, *8* (1), 188−194.
(28) Terzieva, V.; Fransaer, J.; Celis, J. P. *J. Electrochem. Soc.* **2000**, *147* (1), 198−202.
(29) Aslanidis, D.; Fransaer, J.; Celis, J. P. *J. Electrochem. Soc.* **1997**, *144* (7), 2352−2357.
(30) Guglielmi, N. *J. Electrochem. Soc.* **1972**, *119* (8), 1009−1012.
(31) Hovestad, A.; Janssen, L. J. J. Electroplating of Metal Matrix Composites by Codeposition of Suspended Particles. In *Modern Aspects of Electrochemistry*, No. 38; Conway, B. E. et al., Eds.; Kluwer Academic/Plenum Publishers: New York, 2005.
(32) Buelens, C.; Celis, J. P.; Roos, J. R. *J. Appl. Electrochem.* **1983**, *13* (4), 541−548.
(33) Fransaer, J.; Celis, J. P.; Roos, J. R. *J. Electrochem. Soc.* **1992**, *139* (2), 413−425.
(34) Dedeloudis, C.; Fransaer, J. *Langmuir* **2004**, *20* (25), 11030−11038.
(35) Brandes, E. A.; Goldthor, D. *Metallurgia* **1967**, *76* (457), 195−.
(36) Xu, B. S.; Wang, H. D.; Dong, S. Y.; Jiang, B.; Tu, W. Y. *Electrochem. Commun.* **2005**, *7* (6), 572−575.
(37) Stappers, L.; Fransaer, J. *J. Electrochem. Soc.* **2007**, *154* (11), D598−D611.
(38) Stappers, L.; Fransaer, J. *J. Electrochem. Soc.* **2006**, *153* (7), C472−C482.
(39) *Silanes and Other Coupling Agents*, Vol. *5*; Mittal, K. L., Ed.; Koninklijke Brill NV: Leiden, The Netherlands, 2009.
(40) Hu, M.; Noda, S.; Okubo, T.; Yamaguchi, Y.; Komiyama, H. *Appl. Surf. Sci.* **2001**, *181* (3−4), 307−316.
(41) Scola, D. A.; Brooks, C. S. *J. Adhes.* **1970**, *2* (3), 213−237.
(42) Lee, L. H. *J. Colloid Interface Sci.* **1968**, *27* (4), 751−760.
(43) Shao, I.; Vereecken, P. M.; Chien, C. L.; Searson, P. C.; Cammarata, R. C. *J. Mater. Res.* **2002**, *17* (6), 1412−1418.
(44) Shao, I.; Vereecken, P. M.; Cammarata, R. C.; Searson, P. C. *J. Electrochem. Soc.* **2002**, *149* (11), C610−C614.
(45) Tuaweri, T. J.; Wilcox, G. D. *Trans. Inst. Met. Finish.* **2007**, *85* (5), 245−253.
(46) Tuaweri, T. J.; Wilcox, G. D. *Surf. Coat. Technol.* **2006**, *200* (20−21), 5921−5930.
(47) Stöber, W.; Fink, A.; Bohn, E. *J. Colloid Interface Sci.* **1968**, *26* (1), 62−69.
(48) Witucki, G. L. *J. Coat. Technol.* **1993**, *65* (822), 57−60.
(49) Soccol, D.; Martens, J.; Claessens, S.; Fransaer, J. *J. Electrochem. Soc.* **2011**, *158* (8), D515−D523.
(50) Hedberg, J.; Leygraf, C.; Cimatu, K.; Baldelli, S. *J. Phys. Chem. C* **2007**, *111* (47), 17587−17596.